

Dalton Transactions

Accepted Manuscript

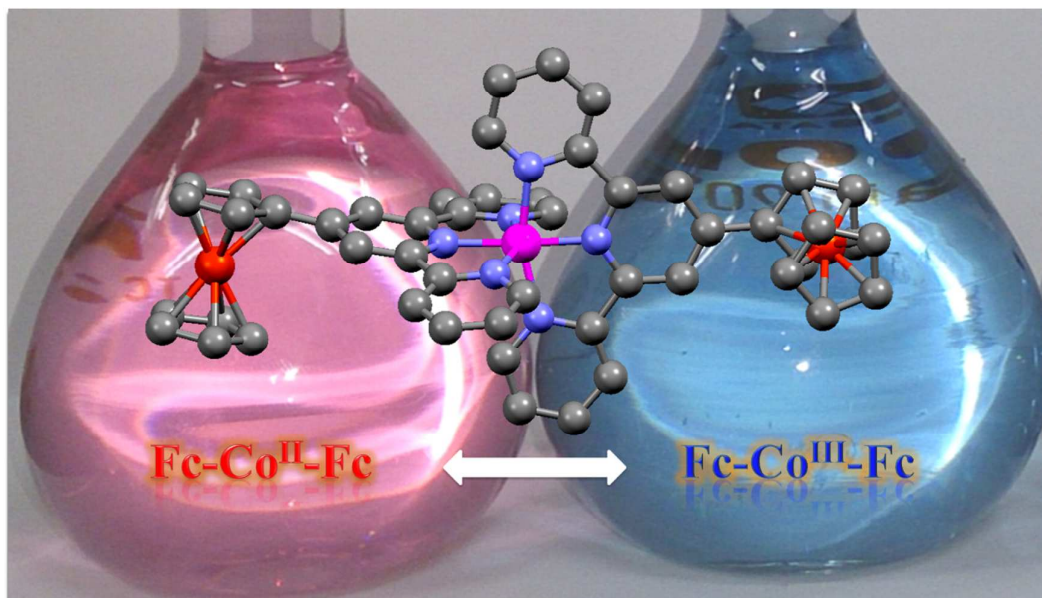


This is an *Accepted Manuscript*, which has been through the Royal Society of Chemistry peer review process and has been accepted for publication.

Accepted Manuscripts are published online shortly after acceptance, before technical editing, formatting and proof reading. Using this free service, authors can make their results available to the community, in citable form, before we publish the edited article. We will replace this *Accepted Manuscript* with the edited and formatted *Advance Article* as soon as it is available.

You can find more information about *Accepted Manuscripts* in the [Information for Authors](#).

Please note that technical editing may introduce minor changes to the text and/or graphics, which may alter content. The journal's standard [Terms & Conditions](#) and the [Ethical guidelines](#) still apply. In no event shall the Royal Society of Chemistry be held responsible for any errors or omissions in this *Accepted Manuscript* or any consequences arising from the use of any information it contains.



Cobalt complexes incorporating ferrocene-terpyridine ligands show a reversible color change between red-violet and blue in response to redox reactions involving the cobalt centers.



Journal Name

ARTICLE

Redox induced colour changes between red-violet and blue in hetero-metal complexes of type $[\text{Co}^{\text{II}}(4'\text{-ferrocenyl-2,2';6'2''-terpyridine)}_2]\text{X}_2$ (X = counter anion)

Received 00th January 20xx,
Accepted 00th January 20xx

DOI: 10.1039/x0xx00000x

www.rsc.org/

Kohei Takami^a, Ryo Ohtani^a, Masaaki Nakamura^a, Takayuki Kurogi^b, Manabu Sugimoto^{*,b,c}, Leonard F. Lindoy^d and Shinya Hayami^{*,a,e}

The hetero-metal complexes $[\text{Co}^{\text{II}}(\text{Fctpy})_2]\text{X}_2$ (Fctpy = 4'-ferrocenyl-2,2';6'2''-terpyridine, X = PF₆ (1) BF₄ (2), ClO₄ (3), BPh₄ (4)) were prepared and their structures and properties were investigated by single crystal X-ray structural analysis, cyclic voltammetry, Mössbauer spectroscopy, UV-vis spectroscopy measurements and DFT calculations. These compounds show reversible redox behaviour in solid state and switching colour between red-violet and blue in response to a change of oxidation state of the cobalt ion centres. $[\text{Co}^{\text{II}}(\text{Fctpy})_2](\text{PF}_6)_2$ (1) and $[\text{Co}^{\text{III}}(\text{Fctpy})_2](\text{PF}_6)_3$ (5) were isolated as the red and blue crystalline products, and the crystal structures were determined. From the results of UV-vis spectroscopy and the DFT calculations, we assigned the respective colours as resulting from MLCT involving the ferrocenyl substituents, with the shift in wavelength of the MLCT reflecting the respective HOMO/LUMO stabilizations induced by the change in oxidation state of the cobalt centres. Furthermore, these compounds 1–4 also showed counter anion-dependent spin crossover behaviours.

Introduction

Colour variation in response to changes of valence and electronic states of metal ions in metal complexes is not only a fundamental property, but is also of importance for the design and construction of molecular devices such as sensors and displays. For example, many spin crossover (SCO) complexes^{1–11} incorporating iron(II),^{3–6} iron(III)³ and cobalt(II)^{4–11} show temperature dependent colour changes accompanied by conversion of their spin states between low-spin (LS) and high-spin (HS). In previous studies we have investigated cobalt(II) terpyridine SCO complexes that show a colour change with change of spin state: LS (orange), HS (yellow). In addition to their SCO behaviour, the cobalt centres are redox (Co^{II}/Co^{III}) active with, in general, the colour of cobalt(III) terpyridine complexes being yellow.^{13–16}

The synthesis of hetero-metal complexes has been a well

exemplified strategy for inducing colour variation in metal complexes, with interactions between the metal ions via bridging organic ligands commonly playing a role in the development of the various colours.^{17–24} Here, we have focused on the use of 4'-ferrocenyl-2,2';6'2''-terpyridine ligand (Fctpy)^{25,26} to synthesize hetero-metal cobalt terpyridine complexes. The ferrocene moiety in the Fctpy metalloligand was anticipated to interact electronically via the terpy group with a cobalt ion bound to the N₃-donor domain of the latter (and vice versa) and be accompanied by a distinct colour change. Modified SCO behaviour for the cobalt complexes was also expected (relative to the corresponding cobalt(II)/terpyridine system). Recently, the Murray group reported a crystal structure of $[\text{Co}^{\text{II}}(\text{Fctpy})_2](\text{ClO}_4)_2$ and its redox behaviour in solution.²⁷ At the same time, we also synthesized and investigated a series of cobalt(II) complexes incorporating the Fctpy ligand in the presence of various counter ions, with our focus on the SCO behaviour of the cobalt centres and the colour changes induced by redox reaction in the solid state.

In this study, we synthesised the cobalt complexes $[\text{Co}^{\text{II}}(\text{Fctpy})_2]\text{X}_2$ (X = PF₆ (1), BF₄ (2), ClO₄ (3), BPh₄ (4)), and investigated their SCO behaviour and solid state redox properties. These compounds show different SCO behaviours depending on the counter anion present. We found that cobalt(II) compounds were red-violet while the corresponding cobalt(III) compounds were blue. The crystal structure of the blue compound, $[\text{Co}^{\text{III}}(\text{Fctpy})_2](\text{PF}_6)_3$ (5), coupled with the results from Mössbauer spectroscopy, UV-vis spectroscopy, and the density functional theory (DFT) calculations indicate

^a Department of Chemistry, Graduate School of Science and Technology, Kumamoto University, 2-39-1 Kurokami, Chuo-ku, Kumamoto 860-8555 Japan.

^b Department of Applied Chemistry and Biochemistry, Kumamoto University 2-39-1 Kurokami, Chuo-ku, Kumamoto 860-8555, Japan.

^c Institute for Molecular Science 338 Nishigo-Naka, Myodaiji, Okazaki 444-8585, Japan.

^d School of Chemistry, the University of Sydney, NSW 2006, Australia.

^e Institute of Pulsed Power Science (IPPS), Kumamoto University, 2-39-1 Kurokami, Chuo-ku, Kumamoto 860-8555 Japan.

Electronic Supplementary Information (ESI) available: Selected bond lengths and angles for 1 and 5, Mössbauer spectra, cyclic voltammograms, results of the DFT calculation. CCDC-1060481–1060482 contains the supplementary crystallographic data for this paper. These data can be obtained free of charge from the Cambridge Crystallographic Data Centre via www.ccdc.cam.ac.uk/data_request/cif

. See DOI: 10.1039/x0xx00000x

the presence of communication between the cobalt centre and the ferrocene substituents via the terpy units.

Results and discussion

$[\text{Co}^{\text{II}}(\text{Fctpy})_2]\text{X}_2$, ($\text{X} = \text{PF}_6$ (**1**), BF_4 (**2**), ClO_4 (**3**), BPh_4 (**4**)) were synthesised by a literature method.²⁶ $[\text{Co}^{\text{III}}(\text{Fctpy})_2](\text{PF}_6)_3$ (**5**) was synthesised by oxidation of **1** using H_2O_2 . The structures of **1** and the oxidised compound **5** were determined by a single crystal X-ray crystallography at 100 K (Fig. 1). Their crystal data and selected bond lengths are shown in Table 1. **1**·**2MeCN** was crystallised in the monoclinic space group $P2_1/n$. The Co-N bond lengths were 2.175(4) Å, 1.940 Å(3), 2.167(4) Å, 1.981(4) Å, 1.870(3) Å and 1.996(4) Å, demonstrating that an elongation of bond lengths occurred in Co(1)-N(1) and Co(1)-N(3) due to Jahn-Teller distortion.² A Cp ring interacts with a hetero ring of terpyridine ligand in a neighboring molecule through a π - π interaction with the internuclear contacts ranging from 3.284 to 3.351, to yield a one dimensional chain structure. A acetonitrile molecule was disordered with being labeled as (N(8)-C(51)-C(52)-N(9)). On the other hand, **5**·**0.75H₂O**·**1.5Acetone** was crystallised in the triclinic space group P-1. The mean Co-N bond length was 1.909 Å which, as expected, is shorter than that for **1** and consistent with the presence of cobalt(III); as shown in Fig. 1(c), three PF_6^- anions were observed per complex cation. In addition to the intermolecular π - π interactions between Cp rings and neighboring terpyridine hetero rings, another intermolecular π - π interaction between Cp rings is present. Average Fe-Cp bond lengths for **1** and **5** are 1.653 Å and 1.642 Å, respectively. These values correspond to that of 1.65 Å for free ferrocene.²⁸

⁵⁷Fe Mössbauer spectroscopy at room temperature was carried out for **1**, **5** and Fctpy (as a control sample) (Fig. S1). In the case of the Fctpy, a wide doublet peak with QS (quadrupole splitting) = 2.33 mms^{-1} and IS = 0.45 mms^{-1} was observed; these values correspond to those reported for (diamagnetic) pristine ferrocene.²⁹ We observed similar wide doublet peaks for **1** (QS = 1.92 mms^{-1} , IS = 0.39 mms^{-1}) and **5** (QS = 1.86 mms^{-1} , IS = 0.38 mms^{-1}), respectively, demonstrating that ferrocene substituent remained intact after the

oxidation of the cobalt(II) to cobalt(III) had occurred in **1**. These results thus corroborated the structural analysis as mentioned above.

We measured the temperature dependent magnetic susceptibilities of **1**–**4** by SQUID under a magnetic field of 1T. Cobalt(II) complexes may show a spin conversion between $S = 3/2$ (t_{2g}^5, e_g^2) and $S = 1/2$ (t_{2g}^6, e_g^1). The molar magnetic susceptibility, $\chi_m T$, of the LS state is about $0.5 \text{ cm}^3 \text{ K mol}^{-1}$, whereas that of the HS state is in the range of 1.9 – $3.5 \text{ cm}^3 \text{ K mol}^{-1}$ due to a contribution from the orbit angular momentum. All the present cobalt(II) compounds exhibited gradual SCO behaviour as shown in Fig. 2; $\chi_m T$ values are in the range 0.375 – $0.523 \text{ cm}^3 \text{ K mol}^{-1}$ at 100 K, which demonstrates that cobalt(II) centres are in the LS state. At 400 K, the $\chi_m T$ values fall in the range of 0.842 – $1.470 \text{ cm}^3 \text{ K mol}^{-1}$. These results reveal that **1**–**4** show incomplete SCO under 400 K; with their transition temperature (T_{\uparrow}) and abruptness being influenced by the size of the counter anions. In the case of **4** (largest anion, BPh_4), T_{\uparrow} was around 100 K, while T_{\uparrow} of **2** (smallest anion, BF_4) was around 290 K. With increasing size of the anions, the T_{\uparrow} decreased and the SCO behaviour became more gradual in accord with the larger counter anions resulting in generally longer intermolecular distances in the complexes, leading to a decrease in their intermolecular interactions.^{5,30} As expected, **5**, consisting of Co^{III} (LS) ions and Fc units, is diamagnetic.

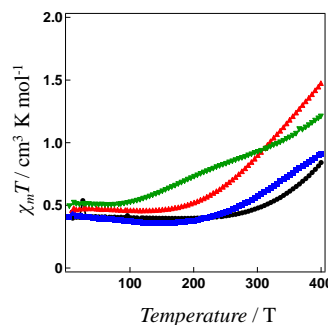


Fig. 2 $\chi_m T$ vs T curves for compounds **1** (red), **2** (black), **3** (blue) and **4** (green).

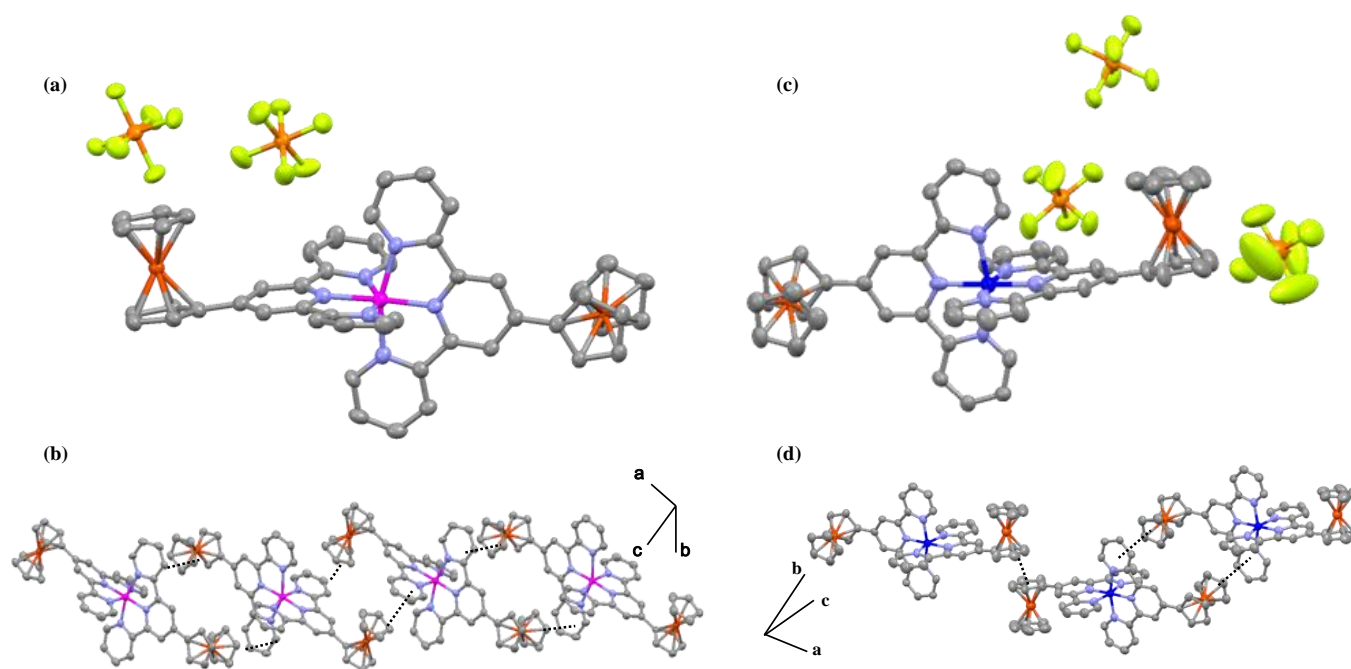


Fig. 1 (a) Molecular structure of **1**·2MeCN. (b) Packing structure of **1**·2MeCN. (c) Molecular structure of **5**·0.75H₂O·1.5Acetone. (d) Packing structure of **5**·0.75H₂O·1.5Acetone. H atoms, solvent molecules are omitted for clarity.

Table 1 Crystal data of **1**·2MeCN and **5**·0.75H₂O·1.5Acetone

| | 1 ·2MeCN | 5 ·0.75H ₂ O·1.5Acetone |
|-------------------------|---|--|
| Formula | C ₅₄ H ₃₁ CoF ₁₂ Fe ₂ N ₈ P ₂ | C ₁₀₉ H ₉₄ Co ₂ F ₃₆ Fe ₄ N ₁₂ O _{4.5} P ₆ |
| Formula weight | 1262.53 | 2863.06 |
| Crystal group | monoclinic | triclinic |
| Space group | P2 ₁ /n | P-1 |
| T (K) | 100 | 100 |
| a (Å) | 12.6847(4) | 12.6886(6) |
| b (Å) | 19.2793(7) | 13.1123(6) |
| c (Å) | 21.2019(7) | 19.4242(10) |
| α (deg) | 90.000 | 81.4130(13) |
| β (deg) | 94.8292(11) | 75.4810(13) |
| γ (deg) | 90.0000 | 71.4120(11) |
| V (Å ³) | 5166.6(3) | 2956.8(2) |
| Z | 4 | 1 |
| ρ (g·cm ⁻³) | 1.623 | 1.608 |
| R1 | 0.0605 | 0.0974 |
| Rw2 | 0.1968 | 0.3483 |
| GOF | 1.110 | 1.068 |

The present compounds have two different kinds of redox active metal centres, cobalt and iron. The redox properties of **1** in the solid state were investigated by solid-state cyclic voltammetry at room temperature as shown in Fig. S2. We applied a standard three-electrode method with glassy carbon as a working electrode, Pt wire counter electrode and Ag/AgCl reference electrode in aqueous

solution. A mixture of **1** and carbon paste was employed as the working electrode and sodium sulfate was used as electrolyte at an ionic strength $I = 0.3$. We observed reversible redox peaks at the following potentials: **1**, $E_{1/2}^I = 0.517$ V vs Ag/AgCl, $E_{1/2}^{II} = 0.143$ V ($E_{1/2} = 1/2(E_{ox} + E_{red})$), $\Delta E^I = 45$ mV and $\Delta E^{II} = 0.186$ V ($\Delta E = E_{ox} - E_{red}$). These peaks are attributed to Fe^{II}/Fe^{III} and Co^{II}/Co^{III}, respectively.³¹ The shift of the redox potential observed for **1** compared with that for pristine ferrocene (black line in Fig. S2) indicates that the ferrocene moieties are stabilised by an electron withdrawing effect by the attached terpyridyl unit.³⁰ Attempts to synthesise the corresponding oxidised (ferrocenium) species using different oxidants such as Ce^{IV}(NH₄)₂(NO₃)₆³² and Fe^{III}(ClO₄)₃³² were unsuccessful because of decomposition after introducing these oxidants.

Interestingly, the cobalt(II) compound **1** is red-violet, on the other hand, the cobalt(III) compound **5** is blue. The solid state (reflection) spectra and UV-vis spectra in acetonitrile solution for **1** and **5** at room temperature are shown in Fig. 3(a). In both spectra, red shifted peaks in the visible region were observed following the formation of **5** by the oxidation of **1**. The UV-vis spectrum of **1** in acetonitrile showed a broad band at 539 nm and sharp band at 316 nm. The broad band was attributed to a MLCT transition involving the iron centre in the Fctpy³¹ unit while the sharp band is assigned to a π - π^* transition in the terpy moieties. On oxidation of **1** to produce **5**, the MLCT band shifted to 596 nm and the π - π^* transition band of the terpy shifted and split to give peaks at 354 nm and 339 nm. The change in oxidation state of the cobalt centre thus impacted on the MLCT band of the ferrocenyl groups via the terpy moieties; this undoubtedly is reflected by the observed colour change between **1** and **5**.

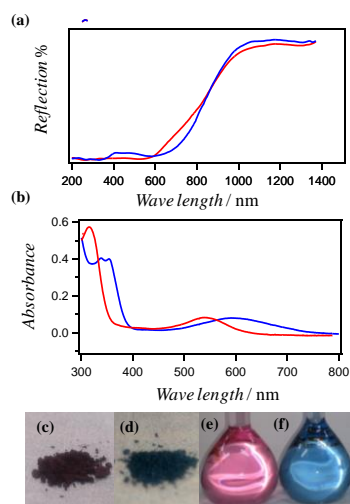


Fig. 3 (a) Solid state reflection spectra for **1** (red) and **5** (blue). (b) UV-vis spectra for 15mM of **1** (red) and **5** (blue) in acetonitrile solution. Photographs of (c) **1** and (d) **5**, and of the acetonitrile solution of (e) **1** and (f) **5**.

In order to elucidate the change in the electronic states between the two oxidation states, we performed DFT calculations for the $[\text{Co}^{\text{II/III}}(\text{Fctpy})]$ complexes in simulated CH_3CN solution where the counter anions were not included, and the time-dependent DFT (TDDFT) method was applied in order to compare the results with the experimental UV-Vis spectra. The details of the excited states and the corresponding valence molecular orbitals describing them are shown in the Supporting Information (Tables S2-S3 and Fig. S3-S5). The theoretically calculated UV-Vis spectra that were shown in Fig. S6 clearly reproduce the experimentally observed spectra except for bands in 400-450 nm regions. As observed experimentally, both the lowest energy band and the most intense band for the $[\text{Co}^{\text{II}}(\text{Fctpy})]$ complex are shifted to lower energies upon its oxidation to $[\text{Co}^{\text{III}}(\text{Fctpy})]$. The calculations also predict that the lowest energy band should appear at 665 nm (1.86 eV) and 641 nm (1.93 eV) for the Co^{III} and Co^{II} complexes, respectively. These are assigned to the experimentally observed bands at 596 nm (2.08 eV) for **5** and at 539 nm (2.30 eV) for **1**, and are attributed to a charge transfer transition from the Fc moiety to the $\text{Co}(\text{tpy})_2$ moiety. The observed shift in spectra upon the oxidation is due to larger stabilisation of unoccupied orbitals than occurs for the occupied orbitals (Fig. 4). These orbital stabilisations for the $[\text{Co}^{\text{III}}(\text{Fctpy})]$ complex reflect the larger positive charge of the Co^{III} ion. As shown in Fig. S3-S5, the LUMO is localised on the $\text{Co}(\text{tpy})_2$ moiety, therefore, this LUMO is more stabilised upon the oxidation than the HOMO localised on the Fc moiety because electrostatic interaction between the Co^{III} ion and the tpy is more effective. For the intense bands in the 300-400 nm region, the calculations predict the occurrence of bands at 3.46 eV (358 nm) and 3.96 eV (313 nm) for the $[\text{Co}^{\text{III}}(\text{Fctpy})]$ and $[\text{Co}^{\text{II}}(\text{Fctpy})]$ complexes, respectively. They correspond to the experimentally observed bands at 354 nm (3.50 eV) for **5** and at 316 nm (3.92 eV) for **1**. This red shift of the band upon the oxidation can be explained in a similar fashion to that for the 641 nm (exptl. 539 nm) band.

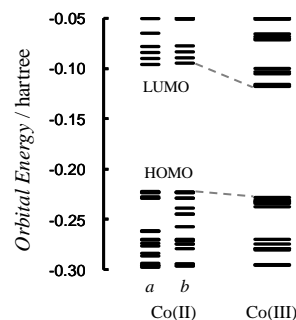


Fig. 4 Orbital energy levels of **1** and **5**. For **1**, spin unrestricted approximation was applied.

Conclusions

We have synthesised the hetero-metal complexes $[\text{Co}^{\text{II}}(\text{Fctpy})_2]\text{X}_2$ ($\text{X} = \text{PF}_6$ (**1**), BF_4 (**2**), ClO_4 (**3**), BPh_4 (**4**)) that show counter anion dependent SCO behaviour and redox properties in the solid state. We obtained the oxidised compound $[\text{Co}^{\text{III}}(\text{Fctpy})_2](\text{PF}_6)_3$ (**5**), and determined the crystal structures of both the cobalt(II) and cobalt(III) compounds, **1** and **5**. Oxidation results in a striking colour change from red-violet for **1** to blue for **5**. The DFT calculations and UV-vis spectra demonstrated that the LUMO is localised on the $\text{Co}(\text{tpy})_2$ moiety in these complexes and is markedly influenced by changing the oxidation state of the cobalt centres, which contributes to observed colour stemming from the MLCT band arising from the Fc substituents. The construction of redox active hetero-metal complexes of present type, in which interactions between metal ions occurs via bridging ligands, clearly represents a useful strategy for influencing the electronic states of the metal centres. Such an approach points the way to new chromophoric materials for potential application in sensor and other electrochromatic devices.

Experimental

Synthesis

The Fctpy ligand and complexes **1**, **2**, **3** and **4** were synthesized by literature methods.²⁶ Complexes **1**–**4** were recrystallised from methanol/acetone to give red-violet plate-like crystals. Single crystals of **1** were obtained by a slow diffusion procedure in acetonitrile/diethyl ether solution. Anal. Calcd for (**1**)-Acetone: C, 51.27; N, 6.77; H, 3.57. Found: C, 51.35; N, 6.96; H, 3.47. Calcd for (**2**)-MeOH·3H₂O: C, 53.12; N, 7.29; H, 4.20. Found: C, 53.00; N, 7.41; H, 3.99. Calcd for (**3**)-2H₂O: C, 53.22; N, 7.45; H, 3.75. Found: C, 53.15; N, 7.48; H, 3.89. Calcd for (**4**)-1.5H₂O: C, 75.50; N, 5.39; H, 5.24. Found: C, 75.59; N, 5.35; H, 5.41. Complex **5** was prepared as follows. A solution of **1** (0.25 g, 0.21 mmol) in a mixture of acetone (20 mL) and acetonitrile (20 mL) was added to 30 %-hydroperoxide (1 mL), NH_4PF_6 (0.13 g, 0.80 mmol) and stirred for 2 days at room temperature to yield a blue solution. This was evaporated to obtain dark-blue powder. The powder was recrystallised from methanol/acetone, washed methanol and dried in vacuo (0.03 g). Anal. Calcd for (**5**)-2H₂O-Acetone: C, 44.75; N, 5.91; H, 3.40. Found: C, 44.92; N, 6.14; H, 3.61.

Physical measurements

X-ray diffraction data for the single crystals were collected at 100 K with a Rigaku R-AXIS RAPID 191R diffractometer. Crystal evaluation and data collection were performed using Cu-K α λ = 1.54187 Å radiation with a detector-to-crystal distance of 1.91 cm. The structures were solved by direct methods and expanded using Fourier techniques. Hydrogen atoms were refined using the riding model. The full-matrix least squares refinements were based on F^2 . The absolute structures were deduced based on the Flack parameter. All calculations were performed using the CrystalStructure crystallographic software (Rigaku) and SHELXL-2013. Elemental analyses (C,H,N) were carried out on a J-SCIENCE LAB JM10 at the Instrumental Analysis Centre of Kumamoto University. The magnetic susceptibilities for **1**, **2**, **3** and **4** between 5K and 400K were measured with a superconducting quantum interference device (SQUID) magnetometer (Quantum Design MPMS-5S) in an external field of 0.5 T. The solid state cyclic voltammetry were measured on a BI-POTENTIostat ALS/DY2323 in aqueous solution of 0.1 M Na₂SO₄ and in 0.1 M tetrabutyl ammonium perchlorate at room temperature. Scan rate of all measurements was 50mV/sec. A standard three-electrode method with glassy carbon as a working electrode, Pt wire counter electrode and Ag/AgCl reference electrode were used. UV spectra of 15mM **1** and **5** in acetonitrile and solid state reflection spectra were recorded with a SCINCO S-2100 spectrophotometer (Shimadzu) at room temperature. The Mössbauer spectra (isomer shift vs metallic iron at room temperature) were measured with a Wissel MVT-1000 Mössbauer spectrometer with a ⁵⁷Co/Rh source in the transmission mode. All isomer shifts are given relative to α -Fe at room temperature. Electronic excited state calculations were carried out by using the time-dependent density functional theory (TDDFT) method. The geometry was taken from the crystallographic data experimentally obtained for **1** and **5**. The M06 functional was used to represent the exchange-correlation functional. The core electrons were described by the Stuttgart (so-called SDD) effective potential for Co and Fe. The valence basis set for the SDD potential for the metal atoms and the 6-31G(d) basis set were used to represent molecular orbitals. In the excited-state calculations, more than 100 excited states were calculated to obtain excitations in the 250-800 nm region. Gaussian band shape with the 3000 cm⁻¹ width was assumed where the band area was equated to the calculated oscillator strength. The solvent effect was taken into account by using the polarizable continuum model (PCM). The present calculations were implemented with the Gaussian09 software.³³

Acknowledgements

This work was supported by JSPS Grant-in-Aid for Young Scientists (B) 15K17833. This work was partially supported by the Cooperative Research Program of 'Network Joint Research Center for Materials and Devices'.

Notes and references

1. J. S. Judge and W. A. Baker Jr., *Inorg. Chim. Acta*, 1967, **1**, 68-72.
2. S. Kremer, W. Henke and D. Reinen, *Inorg. Chem.*, 1982, **21**, 3013-3022.
3. I. Krivokapic, M. Zerara, M. L. Daku, A. Vargas, C. Enachescu, C. Ambrus, P. T. Piggott, N. Amstutz, E. Krausz and A. Hauser, *Coord. Chem. Rev.*, 2007, **251**, 364-378.
4. J. A. Real, A. B. Gasper, V. Niel and M. C. Muñoz, *Coord. Chem. Rev.*, 2003, **236**, 121-141.
5. J. A. Real, A. B. Gasper, V. Niel and M. C. Muñoz, *Dalton Trans.*, 2005, 2062-2079.
6. S. Bonhommeau, G. Molnár, A. Galet, A. Zwick, J. A. Real, J. J. McGarvey and A. Bousseksou, *Angew. Chem., Int. Ed.*, 2005, **44**, 4069-4073.
7. J. Zarembowich, R. Claude and O. Kahn, *Inorg. Chem.*, 1985, **24**, 1576-1580.
8. S. Hayami, M. Nakaya, H. Ohmagari, A. S. Alao, M. Nakamura, R. Ohtani, R. Yamaguchi, T. Kuroda-Sowa and J. K. Clegg, *Dalton Trans.*, 2015, **44**, 9345-9348.
9. S. Hayami, M. R. Karim and Y. H. Lee, *Eur. J. Inorg. Chem.*, 2013, 683-696.
10. S. Hayami, Y. Komatsu, T. Shimizu, H. Kamihata and Y. H. Lee, *Coord. Chem. Rev.*, 2011, **255**, 1981-1990.
11. F. Habib, O. R. Luca, V. Vieru, M. Shiddiq, I. Korobkov, S. I. Gorelsky, M. K. Takase, L. F. Chibotaru, S. Hill, R. H. Crabtree and M. Murugesu, *Angew. Chem., Int. Ed.*, 2013, **52**, 11290-11293.
12. B. Maity, S. Gadadhar, T. K. Goswami, A. A. Karande and A. R. Chakravarty, *Dalton Trans.*, 2011, **40**, 11904-11913.
13. K. B. Aribia, T. Moehl, S. M. Zaakeeruddin and M. Grätzel, *Chem. Sci.*, 2013, **4**, 454-459.
14. C. Enachescu, I. Krivokapic, M. Zerara, J. A. Real, N. Amstutz and A. Hauser, *Inorg. Chim. Acta*, 2007, **360**, 3945-3950.
15. P. Salvatori, G. Marotta, A. Cinti, E. Mosconi, M. Panigrahi, L. Giribabu, M. K. Nazeeruddin and F. D. Angelis, *Inorg. Chim. Acta*, 2013, **406**, 106-112.
16. S. Roy, S. Saha, R. Majumdar, R. R. Dighe, E. D. Jemmis and A. R. Chakravarty, *Dalton Trans.*, 2011, **40**, 1233-1242.
17. U. Siemeling, J. V. D. Brüggem, U. Vorfeld, B. Neumann, A. Stammler, H.-G. Stammler, A. Brockhinke, R. Plessow, P. Zanella, F. Laschi, F. F. d. Biani, M. Fontani, S. Steenken, M. Stapper and G. Gurzadyan, *Chem. Eur. J.*, 2003, **9**, 2819-2833.
18. K. Hutchison, J. C. Morris, T. A. Nile and J. L. Walsh, *Inorg. Chem.*, 1999, **38**, 2516-2523.
19. V. N. Nemykin, A. A. Purchel, A. D. Spaeth and M. V. Barybin, *Inorg. Chem.*, 2013, **52**, 11004-11012.
20. Y. Nishimori, H. Maeda, S. Katagiri, J. Sando, M. Miyachi, R. Sakamoto, Y. Yamanoi and H. Nishihara, *Macromol. Symp.*, 2012, **317**, 276-285.
21. S.-S. Sun and A. J. Lees, *Inorg. Chem.*, 2001, **40**, 3154-3160.
22. T.-Y. Dong, M.-C. Lin, M. Y.-N. Chiang and J.-Y. Wu, *Organometallics*, 2004, **23**, 3921-3930.
23. H. Torieda, A. Yoshimura, K. Nozaki, S. Sakai and T. Ohno, *J. Phys. Chem. A*, 2002, **106**, 11034-11044.
24. P. Comba, G. Linti, K. Merz, H. Pritzkow and F. Renz, *Eur. J. Inorg. Chem.*, 2005, 383-388.
25. A. Juneja, T. S. Macedo, D. R. M. Moreira, M. B. P. Soares, A. C. L. Leite, J. K. D. A. L. Neves, V. R. A. Pereira, F. AVECILLA and A. Azam, *Eur. J. Med. Chem.*, 2014, **175**, 203-210.
26. E. C. Constable, A. J. Edwards, R. Martínez-Mañez, P. R. Raithby and A. M. W. Cargill Thompson, *J. Chem. Soc., Dalton Trans.*, 1994, 645.
27. H. S. Scott, C. J. Gartshore, S. X. Guo, B. Moubaraki, A. M. Bond, S. R. Batten and K. S. Murray, *Dalton Trans.*, 2014, **43**, 15212-15220.
28. J.D. Dunitz, L.E. Orgel and A. Rich, *Acta Crystallogr.*, 1956, **9**, 373-375.

29. R. A. Stukan, S. P. Gubin, A. N. Nesmeyanov, V. I. Goldanskii and E. F. Makarov, *Theor. Exp. Chem.*, 1966, **2**, 581-584.
30. B. Weber, *Coord. Chem. Rev.*, 2009, **253**, 2432-2449.
31. B. Maity, S. Gadadhar, T. K. Goswami, A. A. Karande and A. R. Chakravarty, *Dalton Trans.*, 2011, **40**, 11904-11913.
32. N. G. Connelly and W. E. Geiger, *Chem. Rev.*, 1996, **96**, 877-910.
33. Gaussian 09, Revision D.01, M. J. Frisch, G. W. Trucks, H. B. Schlegel, G. E. Scuseria, M. A. Robb, J. R. Cheeseman, G. Scalmani, V. Barone, B. Mennucci, G. A. Petersson, H. Nakatsuji, M. Caricato, X. Li, H. P. Hratchian, A. F. Izmaylov, J. Bloino, G. Zheng, J. L. Sonnenberg, M. Hada, M. Ehara, K. Toyota, R. Fukuda, J. Hasegawa, M. Ishida, T. Nakajima, Y. Honda, O. Kitao, H. Nakai, T. Vreven, J. A. Montgomery, Jr., J. E. Peralta, F. Ogliaro, M. Bearpark, J. J. Heyd, E. Brothers, K. N. Kudin, V. N. Staroverov, R. Kobayashi, J. Normand, K. Raghavachari, A. Rendell, J. C. Burant, S. S. Iyengar, J. Tomasi, M. Cossi, N. Rega, J. M. Millam, M. Klene, J. E. Knox, J. B. Cross, V. Bakken, C. Adamo, J. Jaramillo, R. Gomperts, R. E. Stratmann, O. Yazyev, A. J. Austin, R. Cammi, C. Pomelli, J. W. Ochterski, R. L. Martin, K. Morokuma, V. G. Zakrzewski, G. A. Voth, P. Salvador, J. J. Dannenberg, S. Dapprich, A. D. Daniels, Ö. Farkas, J. B. Foresman, J. V. Ortiz, J. Cioslowski, and D. J. Fox, Gaussian, Inc., Wallingford CT, 2009.